

RESEARCH

Open Access



# PDE4D drives rewiring of the MAPK pathway in BRAF-mutated melanoma resistant to MAPK inhibitors

Julie Delyon<sup>1,2†</sup>, Selma Becherirat<sup>1†</sup>, Anissa Roger<sup>1</sup>, Mélanie Bernard-Cacchiarella<sup>1,2</sup>, Coralie Reger De Moura<sup>1,3</sup>, Baptiste Louveau<sup>1,3</sup>, Samia Mourah<sup>1,3</sup>, Céleste Lebbé<sup>1,2</sup> and Nicolas Dumaz<sup>1\*</sup>

## Abstract

**Background** Phosphodiesterase type 4D (PDE4D) breaks down cyclic AMP (cAMP) reducing the signaling of this intracellular second messenger which plays a major role in melanocyte pathophysiology. In advanced melanoma, expression of PDE4D is increased, plays a role in tumor invasion and is negatively associated with survival. In the current work, we investigated the role of PDE4D in the resistance of BRAF-mutated melanoma to mitogen-activated protein kinase (MAPK) pathway-targeted therapy.

**Methods** Established human melanoma cell line sensitive and resistant to BRAF and MEK inhibitors and tumor tissues from melanoma patients were used in this study. Immunoblotting was used to analyze protein expression and quantitative reverse transcription-PCR was used to analyze mRNA expression. DNA methylation analysis was evaluated via bisulfite treatment followed by quantitative PCR. Cell viability was measured by clonogenic assays or spheroid cultures. Cell xenograft experiments in immunodeficient mice were used to validate the results in vivo.

**Results** Analysis of baseline tumors from patients with BRAFV600E-mutated melanoma treated with MAPK inhibitors showed that higher PDE4D expression in situ predicted worse survival in patients. Furthermore, acquired resistance to BRAF and MEK inhibitors was associated with overexpression of PDE4D in situ and ex vivo. The overexpression of the PDE4D5 isoform in melanoma cells resistant to targeted therapies was explained by demethylation or deletion of a CpG island located upstream of the PDE4D5 promoter. We further showed that PDE4D overexpression allowed RAF1 activation, promoting a switch from BRAF to RAF1 isoform in BRAF-mutated melanoma, favoring resistance to BRAF and MEK inhibitors. As a result, pharmacological inhibition of PDE4 activity impeded the proliferation of resistant cells ex vivo and in vivo. The anti-tumorigenic activity of PDE4 inhibitor was achieved via inhibition of the Hippo pathway which plays an important role in resistance to targeted therapies.

**Conclusions** In summary, our research showed that PDE4D drives rewiring of the MAPK pathway in BRAF-mutated melanoma resistant to MAPK inhibitors and suggests that PDE4 inhibition is a novel therapeutic option for treatment of BRAF-mutated melanoma patients.

<sup>†</sup>Julie Delyon and Selma Becherirat contributed equally to this work.

\*Correspondence:  
Nicolas Dumaz  
nicolas.dumaz@inserm.fr

Full list of author information is available at the end of the article



**Keywords** Melanoma, Targeted therapy, Resistance, Signal transduction, Phosphodiesterase-4D, RAF kinases

## Background

Metastatic melanoma is the most dangerous skin cancer and a leading cause of cancer in young adults. In approximately half of patients, the tumorigenic processes involve a mutation in the BRAF gene which induces the production of an abnormal BRAF protein constitutively activating the MAPK (mitogen-activated protein kinase) pathway [1]. The discovery of this mechanism fueled the development of targeted therapies to specifically block the action of abnormal BRAF in cancer cells using BRAF and MEK inhibitors. The response to these MAPK inhibitors (MAPKi) is very rapid and sometimes spectacular, with the cessation of tumor progression, but this response is unfortunately brief, with disease recurrence or progression occurring after a median of 11–15 months from the start of treatment due to the development of resistance [2]. The mechanisms of melanoma resistance to MAPKi are still partially understood but the most common mechanism is the re-activation of the MAPK pathway due to rewiring of the signaling pathway, demonstrating that melanoma cells are highly dependent on MAPK pathway activation [3]. MAPK reactivation under MAPKi treatment is often associated with activation of RAF1 (also called CRAF) either because the protein is overexpressed, or because it is activated by RAS, or because it hetero-dimerizes with another kinase of the RAF family [4]. However, the molecular mechanism allowing rewiring of the MAPK pathway in melanoma resistant to therapy is not fully understood.

The RAF kinase family consists of three isoforms, ARAF, BRAF and RAF1, located directly downstream of RAS and upstream of MEK1/2. The RAF family kinases possess a similar structure and can all activate MEK, but are differently regulated by other signaling pathways [5]. For instance, melanocytes use BRAF to activate the MAPK pathway because RAF1 is inhibited by the cAMP pathway in these cells [6, 7]. The very high rate of oncogenic BRAF mutations underlines its fundamental role in melanocyte biology and in melanoma. Nevertheless, while RAF1 did not originally appear to play a major role in melanoma, we and others revealed the importance of this kinase in activating the MAPK pathway in RAS-mutated melanoma [7, 8]. In these cells, BRAF is unable to recruit the MAPK pathway because its phosphorylation by ERK inhibits its interaction with RAS. To escape this negative regulation of BRAF by ERK, melanoma cells carrying a RAS mutation use the RAF1 isoform to activate the MAPK pathway. This rewiring of the MAPK pathway in these melanomas is associated with disrupted cAMP signaling allowing RAF1 activation [9].

cAMP is a second messenger produced in melanocytes downstream of melanotropic hormones such as  $\alpha$ -MSH (alpha-melanocyte stimulating hormone) which binds to the type 1 melanocortin receptor (MC1R). The cAMP pathway is closely associated with melanocyte differentiation, as it stimulates the expression of several specific enzymes involved in melanin synthesis [10]. The cAMP pathway is under the spatiotemporal control of phosphodiesterases (PDE) which constitute the only pathway for degradation of cellular cAMP. There are eight different families of PDEs capable of degrading cAMP and more than 30 different isoforms generated by different promoters and alternative splicing [11]. The isoforms differ by their unique N-terminal end which regulates their cellular localization and modulate their activity [12]. Amongst them, phosphodiesterase 4 (PDE4) constitutes a major component exerting cAMP hydrolytic activity in melanocytes and melanoma. PDE4 enzymes are categorized into four subtypes (PDE4A, PDE4B, PDE4C and PDE4D) whose activity is regulated via their phosphorylation by several kinases, including ERK, allowing signaling cross-talk between the cAMP pathway and the MAPK pathway [13].

We have previously shown that PDE4 activity is increased in RAS mutated melanoma compared to melanocytes, disrupting the cAMP pathway and allowing RAF1 activation [7, 9]. Therefore, as the activation of RAF1 is a mechanism of resistance to MAPKi in BRAF-mutated melanoma, we hypothesized that PDE4 could also be involved in resistance to targeted therapies by MAPKi in BRAF-mutated melanoma. We focused our analysis on PDE4D whose expression is increased in patients with advanced melanoma and has been negatively associated with survival [14, 15]. We show that PDE4D expression is associated with resistance to targeted therapies in BRAF-mutated melanoma patients and is increased in resistant cell lines due to demethylation of a CpG island upstream of the PDE4D5 promoter. PDE4D5 overexpression allows RAF1 activation and increases the number of drug-persistent cells in response to BRAF and MEK inhibitors. PDE4 inhibition impedes the proliferation of resistant cells in vitro and in vivo by inhibiting the hippo pathway.

## Methods

### Patient cohort

A cohort of patients with unresectable advanced melanoma harboring a BRAF V600 mutation were identified from the French prospective MELBASE biobank at Saint-Louis hospital, Paris (ClinicalTrials.gov identifier: NCT02828202, CPP Ile-de-France XI, number 12027,

2012). Patients had been treated with BRAF plus MEK inhibitors, and had available tumor samples taken before starting targeted therapies. All patients provided written informed consent prior to enrollment.

#### Reagents, plasmids and siRNA

Vemurafenib (V600E-BRAF inhibitor), cobimetinib (MEK inhibitor) and decitabine (DNA methyltransferase inhibitor) were obtained from Selleckchem (Houston, TX, USA). pCMV-Flag-YAP-5SA and pCMV-Flag-YAP-5SA/S94A were a gift from Kunliang Guan (Addgene plasmid # 27371; <http://n2t.net/addgene:27371>; RRID: Addgene\_27371 and Addgene plasmid # 33103; <http://n2t.net/addgene:33103>; RRID: Addgene\_33103). For stable YAP expression, YAP-5SA and YAP-5SA/S94A were subcloned in the PEF6/V5-His-TOPO<sup>®</sup> vector (Invitrogen, Cergy Pontoise, France). Melanoma cells were transfected with JetPEI (Polyplus-transfection, Illkirch, France) according to the manufacturer's instructions and cells were selected by blasticidin (10 µg/ml; Sigma Aldrich Chimie, Saint-Quentin-Fallavier, France) for further analysis. Stealth RNAi<sup>™</sup> siRNA targeting BRAF, RAF1 (Supplementary Table 1) or negative controls (Invitrogen, Cergy Pontoise, France) were transfected using Lipofectamine RNAiMAX (Invitrogen, Cergy Pontoise, France) following the manufacturer instructions and cells were lysed after 72 h.

#### Cell culture and proliferation assays

A375, SK-MEL-28 and Dauv1 melanoma cell lines were cultured in RPMI 1640 or DMEM (Invitrogen, Cergy Pontoise, France) containing 10% (v/v) fetal calf serum (FCS; Perbio, Bredières, France), L-glutamin (2 mM; Invitrogen, Cergy Pontoise, France) and antibiotics (100 U/mL of penicillin and 1000 µg/mL of streptomycin; Invitrogen, Cergy Pontoise, France). The identity of the cell lines used in this study was confirmed by NGS. Generation of melanoma cell lines resistant to BRAF and MEK inhibitors were derived from A375, SK-MEL-28 and Dauv1 by culture with increasing doses of vemurafenib up to 10 µM as previously described [16]. Resistant cells are constantly grown in the presence of 10 µM vemurafenib however, for studying the short-term effect of treatments, cells are deprived of serum and vemurafenib 24hrs before treatment. A375 transfected with the empty vector and A375 overexpressing PDE4D5 (A375+PDE4D5) were previously described [15]. For clonogenic assays, melanoma cell lines were seeded at low density and treated 3 times a week with inhibitors or vehicle-only (DMSO) control. Cells were fixed and stained after two weeks with 0.5% (v/v) crystal violet+20% methanol and analyzed. Persister cells were generated by treating A375 cells with vemurafenib and cobimetinib for 72 h. The same number of residual cells were then either plated at a low

density in six-well plates for clonogenic assay or plated in 96 well plates for BrdU assay. BrdU proliferation assay was done using the 5-Bromo-2'-deoxy-uridine Labelling and Detection Kit III (Roche Diagnostics GmbH, Roche Applied Science, Mannheim, Germany) following the manufacturer instructions. For spheroid culture, 2000 cells were seeded in ultra-low-attachment 6-well plates in DMEM/F12 medium supplemented with 1X B27 (Invitrogen, Cergy Pontoise, France), 10 ng/mL of basic fibroblast growth factor (Peprotech, Neuilly-Sur-Seine, France), 20 ng/mL of epidermal growth factor (Peprotech, Neuilly-Sur-Seine, France), and 5 µg/mL of insulin (Sigma Aldrich Chimie, Saint-Quentin-Fallavier, France) and treated with inhibitors or vehicle-only (DMSO) control for 10 days. For EC50 measurement, cells were seeded at 5×10<sup>3</sup> cells/well into a 96-well plate in triplicate and treated with 8 concentrations of inhibitor (from 10 µM to 0.1 nM). Proliferation was monitored using an IncuCyte<sup>®</sup> Live-Cell Analysis System with repeated scanning every 3 h for 72 h (Sartorius, Göttingen, Germany). Growth inhibition and EC50 values for individual compounds were calculated using the IncuCyte<sup>®</sup> software v2019B.

#### RT-qPCR analyses

Total RNA was isolated from frozen or FFPE tissue sections using Trizol reagent (Thermo Fisher Scientific, Waltham, USA) and RNeasy FFPE kit (Qiagen, Hilden, Germany) according to the manufacturer's protocol. RNA quantity and quality were assessed using a NanoDrop ND-1000 spectrophotometer (NanoDrop Technologies, Wilmington, USA). First-strand cDNA was synthesized using a High-Capacity cDNA Archive Kit (Applied-Biosystems) according to the manufacturer's protocol. Transcript levels were measured in duplicate by RT-qPCR using Perfect Master Mix SYBR Green (Thermo Fisher Scientific, Waltham, USA) on LightCycler-480 (Roche). For cultured cells and mouse tumors, total RNA was extracted using Nucleospin RNA kit (MACHEREY-NAGEL GmbH & Co., KG Duren, Germany). First-strand complementary DNA was synthesized using a Go Script Reverse Transcription System (Promega, Madison, WI, USA). Transcript levels were measured in duplicate by RT-qPCR using the Power SYBR Green kit (Applied Biosystems). Transcript levels were normalized using the expression of 2 housekeeping genes, β-ACTIN and β2 microglobulin transcripts. Sequences of primers used for qPCR are in Supplementary Table 1. For RNAseq experiments, cells were treated for 24 h with inhibitors or DMSO control, total RNA was extracted using Nucleospin RNA kit (MACHEREY-NAGEL GmbH & Co., KG Duren, Germany) and the whole transcriptome sequencing was achieved by Integragen (France) and

analysed using the Galileo RNAseq Application. RNAseq data are available upon reasonable request.

#### Promoter reporters and dual-luciferase assay

For reporter luciferase assays a 1541 bp region of the PDE4D locus (chromosome 5 Reference GRCH38.p14: 59770051–59768510) containing the published PDE4D5 promoter [17] was amplified using genomic DNA from A375 cells and cloned into the firefly luciferase vector pGL4.10 vector (Promega, Madison, WI, USA) as described previously [18]. The Renilla luciferase reporter vector pRL-TK was used as a control. Melanoma cells were transfected with JetPEI (Polyplus-transfection, Illkirch, France) according to the manufacturer's instructions and 24 h after transfection, cells were harvested, and dual-luciferase assay was performed using the Dual-Luciferase® Reporter Assay System (Promega, Madison, WI, USA).

#### Western blotting and antibodies

Melanoma cells were lysed using RIPA buffer supplemented with phosphatase and proteinase inhibitor cocktails (PhosSTOP and cComplete Mini, EDTA-free; Roche). Whole-cell lysates were resolved by SDS-polyacrylamide gel electrophoresis and transferred on nitrocellulose membranes. Membranes were probed with the following primary antibodies: Flag,  $\beta$ -ACTIN,  $\alpha$ -ACTININ, p-ERK, ERK, p-MEK, MEK, p259-RAF1, p338-RAF1, p-LATS1 (S909), LATS1, p-YAP1 (S397), YAP1, (Cell Signaling Technology, Danvers, MA, USA), PDE4D (Proteintech), RAF1 (BD Transduction Laboratories), BRAF (Santa Cruz Biotechnology) and p43-RAF1 [7]. Proteins were revealed with a SuperSignal® West Pico Chemiluminescent Substrate (Thermo Scientific, Rockford, IL, USA) on an ImageQuant imaging system and quantified using Image J software (NIH). For measuring its kinase activity, RAF1 was immunoprecipitated from cellular extract and its activity toward MEK was measured in vitro as previously described [9].

#### DNA methylation analysis

To evaluate methylation of the CpG island upstream of the PDE4D5 promoter, the DNA underwent bisulfite conversion of cytosine to uracil. The bisulfite conversion and subsequent purification was performed with the EpiTect Bisulfite kit (Qiagen, Hilden, Germany) according to the manufacturer's instructions. Following bisulfite conversion, the modified DNA template is distinguishable from the original template at methylated cytosines and therefore the methylated sequences are selectively amplified with primers specific for methylation. Bisulfite specific primers that are complementary to the converted DNA were designed using the Methyl Primer Express Software v1.0 (Supplementary Table 1) and the methylated DNA

quantified by qPCR using the Power SYBR Green kit (applied biosystems).

#### Animal studies and treatments

For melanoma cell xenograft experiments, immunodeficient female athymic mice (Swiss-nude), aged 5 weeks, were purchased from Charles River Laboratories (Saint Germain Nuelles, France). The mice were acclimatized for 1–2 weeks before tumor injection. Animal housing, handling and all procedures involving mice were performed in accordance to Directive 2010/63/EU and all protocols were approved by the Committee on the Ethics of Animal Experiments of the French Ministry of Agriculture (Permit Number: APAFIS#11775-2017101316112852 v2). For each treatment procedure, 10 mice were inoculated subcutaneously with  $4 \cdot 10^6$  SK-MEL-28 or SK-MEL-28R1 cells. All the treatments started when tumor volume reached  $80 \pm 30 \text{ mm}^3$ . The size of tumors was assessed with a caliper (large diameter =  $D$  and small diameter =  $d$ ) to obtain the volume  $V = D \times (d)^2 / 2$  twice a week for three weeks. Mice were randomized into groups of 10 mice and treated with control, vemurafenib (10 mg/kg once daily, oral gavage), roflumilast (5 mg/kg once daily, oral gavage) or the combination of both. For in vivo use, vemurafenib was dissolved in 4% DMSO + 30% PEG 300 + 5% Tween 80 whereas roflumilast was dissolved in 30% PEG400 + 0.5% Tween80 + 5% propylene glycol according to Manufacturer's instructions.

#### Statistical analysis

Statistical analyses for in vitro and in vivo data were performed with GraphPad Prism v6.0 software (GraphPad, San Diego, CA) using the Student's *t*-test. All data are expressed as mean  $\pm$  standard deviation (SD) from at least three independent experiments. For patient data, statistical analyses were performed with R (R Foundation for statistical computing, Vienna Austria). The median value of PDE4D expression measured by quantitative RT-PCR was 10.27 (PDE4D/b2m  $\times 10^{11}$ ). All group comparisons were done using one-way ANOVA followed by Tukey post-hoc test. All statistical tests were considered to be significant when *P*-values lower than 0.05 were obtained. Progression free survival was estimated with the Kaplan Meier method and comparison was assessed with the log-rank test.

## Results

### PDE4D is overexpressed in melanoma and cell lines resistant to targeted therapies

To gain insight into the involvement of PDE4D in resistance to targeted therapies, we first analyzed the expression levels of PDE4D at baseline in a panel of 31 human melanoma biopsy samples from patients with metastatic melanoma treated with BRAF and MEK inhibitors. We

showed that PDE4D expression at baseline is associated with poor progression-free survival (PFS) in patients treated with targeted therapies (Fig. 1A,  $P=0.043$ ). In 2 patients for whom we had biopsies before treatment and at resistance, we observed that PDE4D expression increased upon treatment suggesting a correlation

between overexpression of PDE4D and acquired resistance to treatment (Fig. 1B).

To evaluate this hypothesis in vitro, we established experimental models of BRAF mutated melanoma cell lines with acquired resistance to BRAF (vemurafenib) and MEK (cobimetinib) inhibitors. From each parental cell line, A375 and SK-MEL-28, we derived two independent

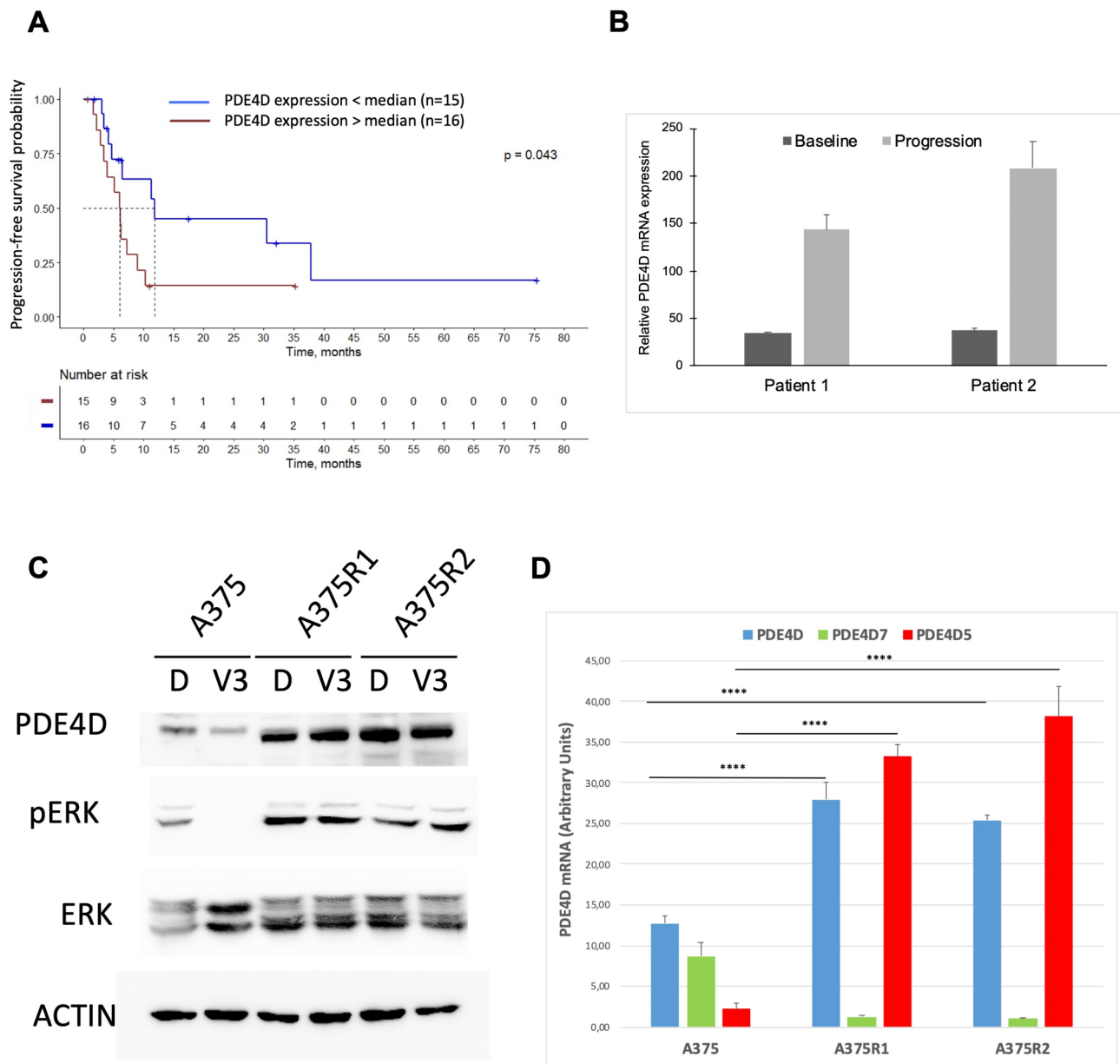


**Fig. 1** PDE4 expression is associated with response to BRAFi + MEKi in BRAF-mutated melanoma. **A** Progression-free survival probability in advanced melanoma patients treated with BRAFi + MEKi ( $n = 31$ ) according to the mRNA expression of PDE4D in tumor samples (below the median range,  $n = 15$ , blue; above the median range,  $n = 16$ , red). **B** Relative mRNA expression of PDE4D in tumors at baseline (black) and at progression (white) upon BRAFi + MEKi from 2 advanced melanoma patients with a median expression of PDE4D. **C** A375 and its resistant derivatives A375R1 and A375R2 were treated with vemurafenib 3  $\mu$ M (V3) or DMSO (D) as a control for 24 h. The effect on PDE4D expression and ERK phosphorylation (pERK) was measured by immunoblot, total ERK and  $\beta$ -ACTIN served as a loading control. **D** mRNA level of total PDE4D as well as PDE4D7 and PDE4D5 isoforms was quantified by quantitative by RT-PCR, normalized to GAPDH mRNA level, in A375 and its resistant derivatives A375R1 and A375R2. Bars represent mean  $\pm$  SD and results are representative of 3 independent experiments per line, \*\*\*\*  $P < 0.0001$ ; unpaired Student t-test

resistant cell lines, A375R1 and A375R2, and SK-MEL-28R1 and SK-MEL-28R2, by selective growth in a medium containing increasing concentrations of the BRAF inhibitor. To evaluate the resistance of these cell lines to MAPKi, we measured the EC<sub>50</sub> of vemurafenib and cobimetinib for the proliferation of parental and resistant cell lines. A375R1 and A375R2 showed a 20-to-50-fold increased resistance to vemurafenib and a 20-to-45-fold increased resistance to cobimetinib in comparison to A375 parental cell line. SK-MEL-28R1 and SK-MEL-28R2 showed a 120-to-180-fold increased resistance to vemurafenib and a 17-to-30 fold increased resistance to cobimetinib in comparison to SK-MEL-28 parental cell line (Supplemental Table 2). Next, we analyzed protein expression of PDE4D in melanoma cell lines sensitive or resistant to BRAF and MEK inhibitors. A375R1 and A375R2 resistant cells exhibited a markedly increased expression of PDE4D relative to the parental cell line (Fig. 1C, D). Interestingly, parental SK-MEL-28 presented a high level of PDE4D expression which was not significantly increased in resistant SK-MEL-28R1 and SK-MEL-28R2 cells (Supplemental Fig. 1A). We therefore established resistant cells from a third BRAF-mutated cell line called Dauv1 which expressed a low level of PDE4D, and showed that Dauv1R1 and Dauv1R2 resistant cells exhibited a markedly increased expression of PDE4D relative to the parental cell line, similar to that observed in resistant A375 cells (Supplemental Fig. 1B). To understand the mechanism of resistance to MAPK inhibition, A375 parental and resistant cells were treated with 3  $\mu$ M vemurafenib and the effect on ERK phosphorylation was evaluated by Western blot. Western blot analyses revealed that ERK phosphorylation was strongly reduced in parental A375 cells treated with vemurafenib. However, in A375R1 and A375R2 resistant cells, phosphorylation was maintained despite treatment with vemurafenib (Fig. 1C) demonstrating that resistance was associated with reactivation of the MAPK pathway in these cells. Similar results were obtained with SK-MEL-28 and Dauv1 (Supplementary Fig. 1). We used reverse transcription followed by real-time PCR to identify the PDE4D isoforms expressed in parental and resistant melanoma cells. We found that A375 resistant cell lines not only expressed more PDE4D than parental cells, but they also expressed different isoforms. Using specific probes, we found that parental A375 cells expressed mainly the PDE4D7 isoform, whereas resistant A375R1 and A375R2 cells expressed the PDE4D5 isoform (Fig. 1D). A similar increase in PDE4D5 expression was observed in resistant DAUV1R1 and DAUV1R2 cells compared to parental DAUV1 cells (Supplemental Fig. 1C). Parental SK-MEL-28 cells already mainly expressed the PDE4D5 isoform, and its expression was only slightly increased in

resistant SK-MEL-28R1 and SkMMel28R2 cells (Supplemental Fig. 1C).

Following these results, we evaluated the expression of the PDE4D5 isoform in the panel of human melanoma biopsy samples which had been previously analyzed. We showed a tendency for an association of PDE4D5 expression with shorter PFS, although the difference was not statistically significant (Supplemental Fig. 2A). We also observed that PDE4D5 expression increased upon treatment for the 2 patients for which we had biopsies before and after treatment (Supplemental Fig. 2B) suggesting that expression of the PDE4D5 isoform is, at least partially, associated with resistance to treatment.

### **Methylation of a CpG island upstream of the PDE4D5 promoter inhibits its activity**

Because the PDE4D5 isoform possesses its own promoter, we investigated the activity of this promoter in the different cell lines to try to understand the differing expression of PDE4D5 between A375, Dauv1 and SK-MEL-28 cells, and between sensitive (parental) and resistant A375 cells. We first sequenced the PDE4D5 promoter in sensitive and resistant SK-MEL-28 and A375 cells, and did not find any genetic variation from the published sequence which could explain the difference in expression (data not shown). To evaluate the activity of this promoter in cells expressing different level of PDE4D5, we cloned the 1541 bp long promoter in front of a luciferase reporter gene and transfected the constructs in A375, Dauv1 and SK-MEL-28 cells. The PDE4D5 promoter induced a strong luciferase activity compared to the vector lacking the promoter element, demonstrating the strong activity of the PDE4D5 promoter in all cell lines (Fig. 2A). The robust activity of the PDE4D5 promoter in parental A375 cells which do not express significant level of PDE4D5 suggests that epigenetic mechanisms may inhibit the endogenous PDE4D5 promoter accessibility in these cells. Epigenetic modifications could also explain the difference in expression of PDE4D5 in sensitive versus resistant A375 cells. In accordance, we identified a CpG island upstream of the PDE4D5 promoter suggesting a possible role for methylation in controlling PDE4D5 expression (Fig. 2B). Interestingly, this CpG island is located in a region of chromosome 5 which was described as deleted in SK-MEL-28 (Fig. 2B) but not in A375 cells. We first confirmed the deletion of this fragment in our SK-MEL-28 cell line by next generation sequencing (data not shown) reinforcing the importance of this region in inhibiting the PDE4D5 promoter. To test this hypothesis, we treated the cells with decitabine (DAC), a DNA-demethylating agent, and quantified expression of PDE4D5 by quantitative RT-PCR. DAC induced a significant increase in PDE4D5 expression in A375 and Dauv1 cells but not in

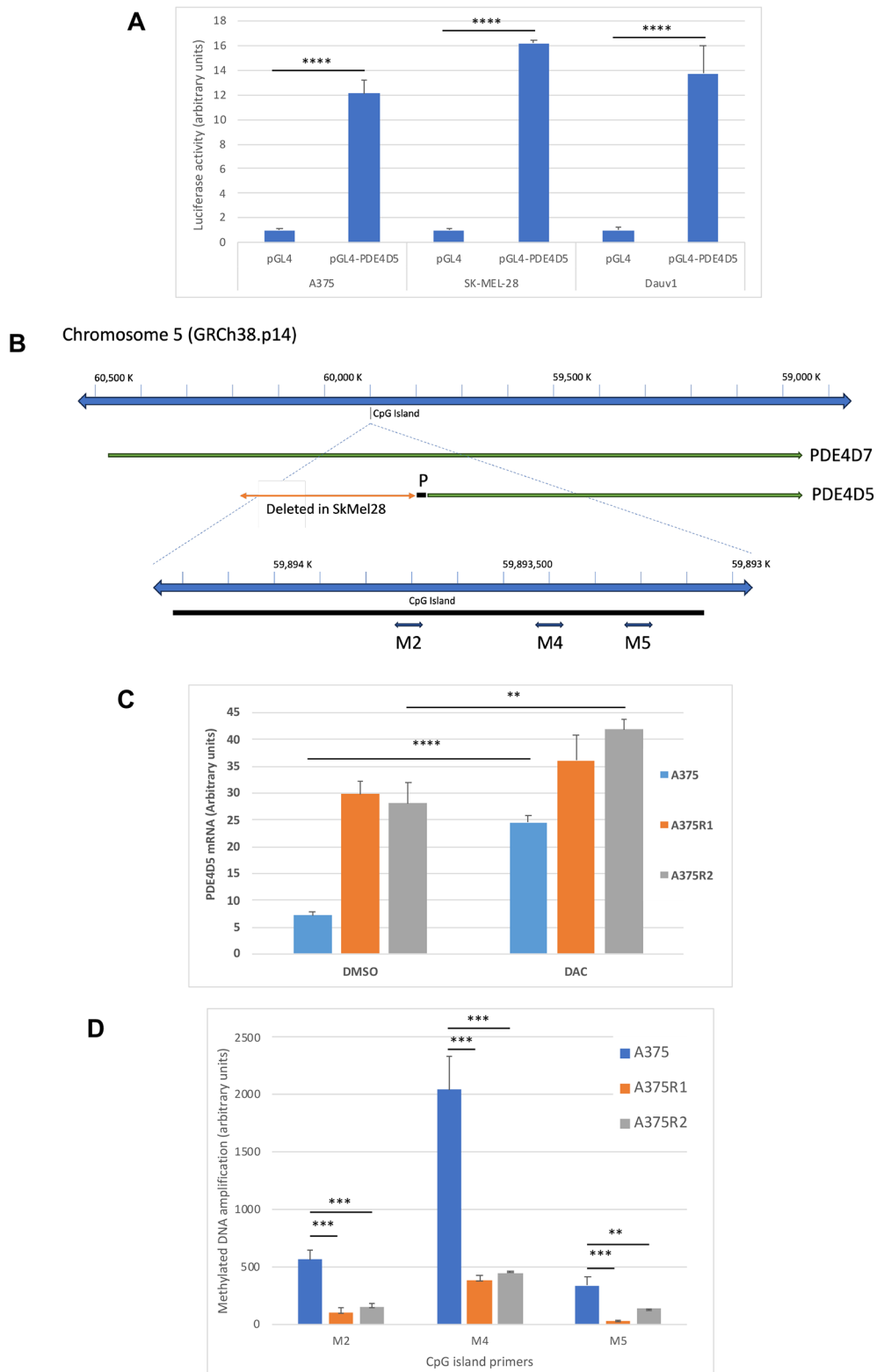


**Fig. 2** (See legend on next page.)

(See figure on previous page.)

**Fig. 2** Methylation of a CpG island upstream of the PDE4D5 promoter inhibits its activity. **A** Luciferase reporter construct containing the PDE4D5 promoter sequence (pGL4-PDE4D5) was transfected in triplicate into A375, Dauv1 and SK-MEL-28 cell lines. The construct without the promoter used as a control (pGL4). Cells were harvested 24 h post transfection and reporter expression was analyzed using the Dual-Luciferase assay system. **B** Schematic representation of the PDE4D locus on chromosome 5. The PDE4D5 promoter is indicated by P, the sequence deleted in SK-MEL-28 is indicated by an orange arrow, the CpG island is indicated by a black line and the 3 regions amplified for analyzing DNA methylation are indicated below the line (M2, M4 and M5). **C** mRNA level of the PDE4D5 isoform was quantified by quantitative by RT-PCR, normalized to GAPDH mRNA level, in A375 and its resistant derivatives A375R1 and A375R2 treated 24 h with DMSO or decitabine (DAC). **D** the DNA extracted from A375, A375R1 and A375R2 underwent bisulfite conversion of cytosine to uracil and the methylated sequences were selectively amplified with primers specific for methylation at 3 sites in the CpG island (M2, M4 and M5) by qPCR. Bars represent mean $\pm$ SD and results are representative of 3 independent experiments per line.  $^{**}P < 0.01$ ,  $^{***}P < 0.001$ ,  $^{****}P < 0.0001$ ; unpaired Student t-test

SK-MEL-28 cells which already expressed a significantly higher level of PDE4D5 (Supplementary Fig. 2C). Moreover, whereas DAC induced a significant increase in PDE4D5 expression in A375 parental cells it only induced a slight increase in resistant cells (Fig. 2C) suggesting that methylation may inhibit the PDE4D5 promoter in sensitive A375 cells but not resistant ones. To compare the methylation status of the CpG island in sensitive versus resistant A375 cells, we used bisulfite treatment followed by quantitative PCR. We used primer couples located at different sites on the CpG island (Fig. 2B). For each set of primers, the results showed a significantly higher methylation level in sensitive parental A375 cells compared to resistant A375R1 and A375R2 cells, confirming a role of methylation at this CpG island in regulating PDE4D5 expression. Demethylation of the CpG island, or its deletion, could therefore explain the expression of PDE4D5 in melanoma cells resistant to targeted therapies.

#### PDE4D overexpression activates RAF1

We have previously shown that PDE4 activity is increased in RAS mutated melanoma to promote a switch from the BRAF to RAF1 isoform in the MAPK pathway [9]. We therefore hypothesized that overexpression of PDE4D in resistant cells could promote RAF1 activation, allowing MAPK activation in these cells in the presence of a MAPKi. To first evaluate the importance of RAF1 in MAPK activation in resistant cells, we used siRNA to specifically inhibit BRAF or RAF1 isoforms in sensitive and resistant A375 cells. As expected, when RAF1 was depleted in A375 parental cells, ERK activity was not affected whereas it was strongly inhibited (77%) when BRAF was depleted (Supplemental Fig. 3). Interestingly, however, when RAF1 was depleted in A375R1 and A375R2 resistant cells, ERK activity was significantly inhibited by around 50% whereas BRAF depletion did not affect ERK activation in these cells (Supplemental Fig. 3). These results demonstrate that it is RAF1, rather than BRAF, which is required for ERK activity in resistant cells. To investigate whether PDE4D overexpression is able to regulate RAF1 activity in BRAF-mutated cells, we overexpressed PDE4D5 in A375 sensitive cells and measured RAF1 phosphorylation and activity. PDE4D5 overexpression induced a reduction of RAF1 phosphorylation

on S43 and S259, which are known to be phosphorylated by the protein kinase A (PKA) downstream of the cAMP pathway and known to inhibit RAF1 activity. In contrast, an increase in S338 phosphorylation known to be associated with RAF1 activation was observed in cells overexpressing PDE4D5 (Fig. 3A). To confirm the increase in RAF1 activity associated with these phosphorylation events, RAF1 was immunoprecipitated and its kinase activity against MEK measured *in vitro*. A significant 2-fold increase in RAF1 activity was observed in PDE4D5 expressing cells compared to parental cells leading to increased ERK phosphorylation in A375+PDE4D5 cells (Fig. 3B and Supplementary Fig. 4A). On the contrary when PDE4D was inhibited by roflumilast, a PDE4 inhibitor, RAF1 kinase activity was significantly reduced (Fig. 3B and Supplementary Fig. 4A), demonstrating that PDE4D overexpression is able to regulate RAF1 activity by inhibiting the cAMP pathway. To evaluate whether PDE4D can promote a switch from BRAF to RAF1 isoform in BRAF mutated cells, we evaluated the importance of RAF1 in MAPK activation in cells overexpressing PDE4D5. We used siRNA to specifically inhibit BRAF or RAF1 isoforms in parental A375 cells and in the resistant cells overexpressing PDE4D5. RAF1 depletion significantly reduced ERK activity by around 50% in the resistant cells whereas the reduction of activity was not significant in parental A375 cells. ERK activity was strongly (90%) inhibited in both cell lines by BRAF depletion (Fig. 3C). Taken together, our results suggest that although PDE4D5 overexpression cannot promote a complete switch from BRAF to RAF1 isoform, it increases RAF1 activation and supports its contribution to MAPK activation in BRAF-mutated cells.

#### PDE4D5 overexpression increases drug-tolerant persister cells

To evaluate whether RAF1 activation induced by PDE4D5 overexpression could induce resistance to MAPKi, we compared the EC<sub>50</sub> of vemurafenib and cobimetinib for the proliferation of parental A375 and resistant cell lines. Overexpression of PDE4D5 induced a 6-fold increased resistance to vemurafenib and a 2-fold increased resistance to cobimetinib in comparison to the A375 parental cell line (Sup Table 2). When RAF1 was silenced by



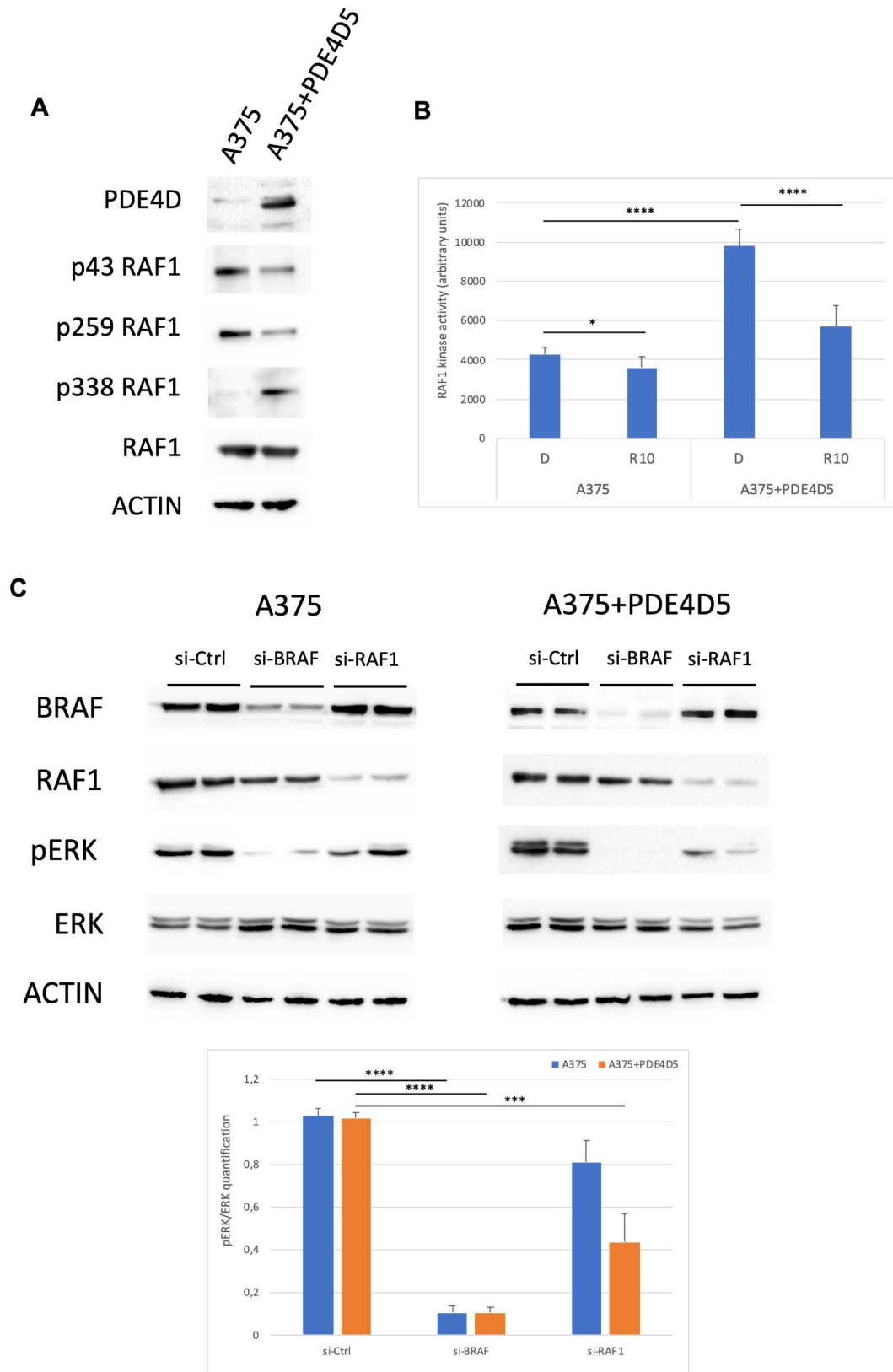


**Fig. 3** (See legend on next page.)

(See figure on previous page.)

**Fig. 3** PDE4D induced RAF1 reactivation in BRAF mutated melanoma cell lines. **A** Expression of PDE4D and phosphorylation of RAF1 on S43 (p43), S259 (p259) and S338 (p338) in A375 transfected with empty vector and A375 overexpressing PDE4D5 (A375 + PDE4D5). Total RAF1 served as a loading control. **B** RAF1 was immunoprecipitated from A375 transfected with empty vector and A375 overexpressing PDE4D5 (A375 + PDE4D5) treated for 24 h with DMSO (D) or 10 $\mu$ M Roflumilast (R10) and its kinase activity toward MEK measured in vitro. Quantification of the phosphorylated MEK (pMEK) signal normalized to total MEK signal is presented as mean  $\pm$ SD and results are representative of 3 independent experiments per line. **C** A375 transfected with empty vector and A375 overexpressing PDE4D5 (A375 + PDE4D5) were transfected with siRNA control (si-Ctrl), targeting BRAF (si-BRAF) or RAF1 (si-RAF1) siRNA. The effect on BRAF and RAF1 expression and on ERK phosphorylation (pERK) was measured by immunoblot, total ERK served as a loading control. Quantification of the pERK signal normalized to total ERK signal is presented below the blots as mean  $\pm$ SD and results are representative of 3 independent experiments per line. \* $P < 0.05$ , \*\*\* $P < 0.001$ , \*\*\*\* $P < 0.0001$ ; unpaired Student t-test

siRNA in resistant cells, the EC<sub>50</sub> of vemurafenib and cobimetinib was reduced back to that observed in the parental A375 cells (Supplementary Fig. 4B). These data demonstrate that PDE4D5 induces a partial resistance to BRAF and MEK inhibitors by activating RAF1. We also evaluated the ability of PDE4D5 overexpression to increase the formation of drug-tolerant persister cells, which are a reservoir for resistant cells. We exposed parental A375 and resistant cell lines to lethal concentrations of vemurafenib or cobimetinib. After 72 h of treatment, most of the cells had died and only a small fraction of drug-tolerant cells remained. We evaluated the residual ERK activity in these cells and observed a significant 2-fold increase in residual ERK phosphorylation compared to parental A375 cells (Fig. 4A). We evaluated the capacity of the remaining cells to proliferate using BrdU and showed that although vemurafenib and cobimetinib were cytotoxic in both cell lines, PDE4D5 overexpression significantly increased proliferation (Fig. 4B). We also compared the ability of these drug-tolerant persister cells to form colonies using a clonogenic assay. We observed that overexpression of PDE4D5 significantly increased by 2-fold the formation of clones by drug-tolerant persister cells (Fig. 4B). Together, these results demonstrate that by increasing RAF1 activity in BRAF-mutated cells, PDE4D5 induces a partial resistance of the MAPK pathway to BRAF and MEK inhibitors. This leads to an increase in drug-tolerant persister cells which could favor the emergence of resistant clones after genetic alterations.

#### **PDE4 inhibition reduces proliferation of MAPKi-resistant melanoma cells in vitro and in vivo**

To gain insight into the therapeutic potential of targeting PDE4D in melanoma resistant to targeted therapies, we evaluated the effect of the PDE4 inhibitor roflumilast on melanoma proliferation. A375 and SK-MEL-28 cells and their resistant derivatives R1 and R2 were treated with roflumilast alone or combined with vemurafenib, and the effect on colony formation was evaluated. We confirmed that A375R1, A375R2, SK-MEL-28R1 and SK-MEL-28R2 cells were resistant to treatment with vemurafenib (Fig. 5A). However, roflumilast reduced colony formation by 36–39% for A375R1 and A375R2 cells, and by 54–72% for SK-MEL-28R1 and SK-MEL-28R2 cells. The combination of vemurafenib and roflumilast further

inhibited colony formation by 87–91% for A375R1 and A375R2 cells, and by 67–89% for SK-MEL-28R1 and SK-MEL-28R2 cells (Fig. 5A). We confirmed these results on Dauv1 and their resistant derivatives R1 and R2 with the particularity that Dauv1R1 and Dauv1R2 are dependent on vemurafenib for growth and therefore do not form colonies in absence of vemurafenib (Supplementary Fig. 5). However, the combination of vemurafenib and roflumilast reduced colony formation by 80% for Dauv1R1 and Dauv1R2 cells compared to vemurafenib alone.

Formation of spheroids by tumor cells cultured in non-adherent conditions has been described as a characteristic of less differentiated cancer cells with a higher ability to form tumors. Spheres are enriched in cells with characteristics of tumor initiating cells [19, 20], which are involved in recurrence and drug resistance [21]. Therefore, we cultivated BRAF-mutated melanoma cells as spheroids to uphold the effects of PDE4 inhibition in a model more representative of tumor growth than cells grown as monolayers. Parental and resistant A375 and SK-MEL-28 cells grown as melanospheres were treated with roflumilast alone or in combination with vemurafenib. We showed that the sphere size of parental and resistant cells was significantly reduced by roflumilast monotherapy as well as in combination with vemurafenib (Fig. 5B). In resistant cells, while vemurafenib alone increased sphere size, the combination of roflumilast and vemurafenib reduced sphere growth by 52–84% for A375R1 and A375R2 cells, and by 90% for SK-MEL-28R1 and SK-MEL-28R2 cells compared to vemurafenib alone (Fig. 5B).

In light of these ex vivo results, we next investigated whether the PDE4 inhibitor could inhibit tumor growth in vivo. We grafted parental and resistant SK-MEL-28 cells in nude mice because these cells express the highest level of PDE4D and showed the best response ex vivo. Once the tumor reached 80 $\pm$ 30 mm<sup>3</sup> the mice were treated with vemurafenib, roflumilast or the combination of both and the tumor growth was monitored regularly. After 21 days, we observed an inhibition of SK-MEL-28 parental cell tumor size by vemurafenib or roflumilast alone, although this was not significant. However, the combination of vemurafenib and roflumilast induced a significant reduction in SK-MEL-28 parental cell tumor

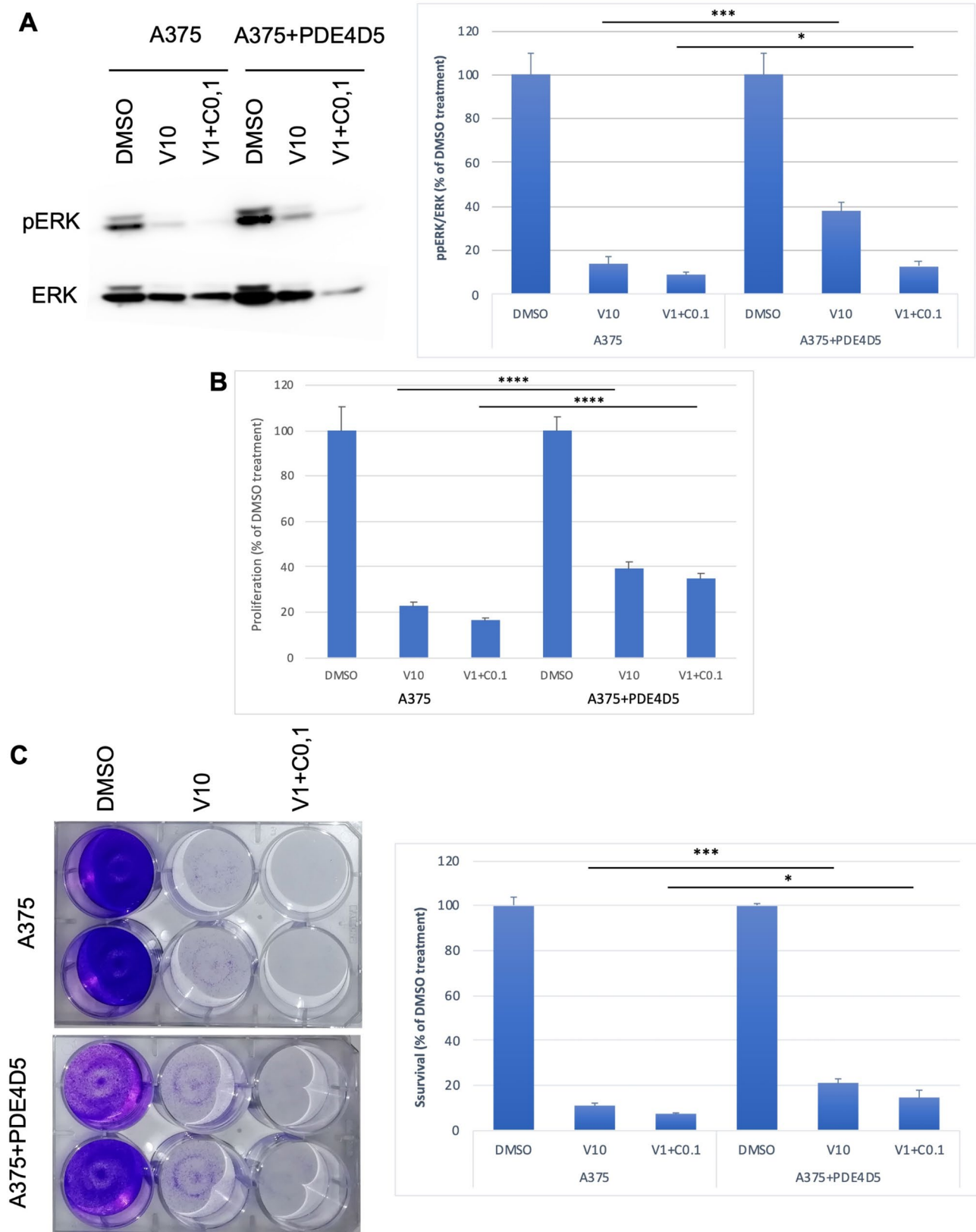


**Fig. 4** (See legend on next page.)

(See figure on previous page.)

**Fig. 4** PDE4D5 overexpression increases drug-resistant persister cells. **A** parental A375 and A375 + PDE4D5 cell lines were treated with 10  $\mu$ M vemurafenib (V10), a combination of 1  $\mu$ M vemurafenib and 0.1  $\mu$ M cobimetinib or DMSO control for 72 h. ERK phosphorylation (pERK) was measured by immunoblot in the fraction of drug-resistant cells remaining, total ERK served as a loading control. Quantification of the ratio pERK/ERK on non-saturating blots is shown beside the blot as mean  $\pm$  SD and results are representative of 3 independent experiments per line. **B** and **C** parental A375 and A375 + PDE4D5 cell lines were treated with 10  $\mu$ M vemurafenib (V10), a combination of 1  $\mu$ M vemurafenib and 0.1  $\mu$ M cobimetinib or DMSO control for 72 h and the ability of these drug-resistant persister cells to proliferate was evaluated by BrdU labeling (**B**) or clonogenic assay (**C**). Bars represent mean  $\pm$  SD and results are representative of 3 independent experiments per line. \* $P < 0.05$ , \*\*\* $P < 0.001$ , \*\*\*\* $P < 0.0001$ ; unpaired Student t-test

size compared to the control group ( $P = 0.01$ ; Fig. 5C and Supplemental Fig. 7). The SK-MEL-28R1 cells formed tumors resistant to vemurafenib treatment. While roflumilast alone only slightly reduced the size of tumor after 18 days of treatment, the combination of vemurafenib and roflumilast induced a significant reduction in SK-MEL-28R1 cell tumor size compared to the vemurafenib alone group ( $P = 0.02$ ; Fig. 5C and supplementary Fig. 7A).

#### PDE4 inhibition suppresses melanoma growth through inactivation of the Hippo pathway

Next, we sought to determine the molecular mechanism by which the PDE4 inhibitor, roflumilast, inhibited melanoma growth. The significant reduction of cell viability by the combination of roflumilast and vemurafenib in resistant cells prompted us to first investigate the canonical oncogenic pathways, PI3K/AKT and MAPK/ERK. Interestingly, our results showed no effect of the inhibitors on ERK or AKT phosphorylation in any of the cell lines (data not shown). To better understand the impact of PDE4 inhibition, we then compared the mRNA expression profiles between control samples and vemurafenib or roflumilast treated samples. A RNA seq analysis was done on A375, A375R1, SK-MEL-28 and SK-MEL-28R1 cells after 24 h of treatment with vemurafenib, roflumilast and the combination of both. We used a previously described melanoma BRAFV600E signature [22] and confirmed that expression of these genes was modified by vemurafenib in parental A375 and SK-MEL-28 cell lines but not in resistant A375R1 and SK-MEL-28R1 cells (Supplementary Fig. 8A). In contrast, roflumilast had no effect on the BRAFV600E signature in parental or resistant cell lines confirming that PDE4 inhibitor did not act on the MAPK pathway (Supplementary Fig. 8A).

Because recent work showed that cAMP acts as a tumor suppressor in a wide range of human cancers through inactivation of the Hippo protein YAP [23], we evaluated the effect of roflumilast on a melanoma YAP signature [24]. We first showed that expression of these genes was increased in resistant cells compared to parental cells confirming the activation of the Hippo/Yap pathway in resistant melanoma cell lines (Supplementary Fig. 8B). Furthermore, this analysis revealed a general inhibition of expression of genes associated with the Hippo pathway in melanoma cells treated with the PDE4 inhibitor (Fig. 6A and supplementary Fig. 8B). In resistant A375R1 and SK-MEL-28R1 cells, the effect on

the Hippo/YAP signature was stronger when combining vemurafenib with roflumilast (Fig. 6A and supplementary Fig. 8B). To confirm this observation, we measured by quantitative RT-PCR the expression of the canonical Hippo pathway-dependent genes, CCN1 (also known as CYR61) and CCN2 (also known as CTGF) and observed a significant reduction in expression of both YAP target genes in response to roflumilast (Fig. 6B). We also evaluated CCN1 and CCN2 mRNA expression by quantitative RT-PCR in SK-MEL-28R1 cell tumors treated with vemurafenib alone or the combination of vemurafenib and roflumilast. We observed a significant reduction of CCN1 expression in tumors treated with roflumilast and a decrease, although not significant, of CCN2 in tumors treated with the PDE4 inhibitor (Supplementary Fig. 7B). Because these findings suggested that roflumilast suppressed cell growth by preventing YAP activation, we measured phosphorylation of YAP and its upstream kinase LATS1 in parental and resistant cells. Treatment of cells with roflumilast induced the phosphorylation of LATS1 and the concomitant phosphorylation of its target YAP. Numerous studies have established that most upstream signals regulate YAP activity by influencing its phosphorylation, abolishing YAP binding to 14-3-3 and increasing its nuclear localization. Therefore, the phosphorylation of YAP has been widely recognized as an indicator of its cellular localization and inactivation [25]. Taken together, our results suggest that roflumilast suppresses cell growth by activating cAMP-PKA mediated activation of LATS1 leading to YAP phosphorylation and inhibition. To confirm the role of YAP phosphorylation in roflumilast-mediated cell growth suppression, A375R1 and SK-MEL-28R1 cell lines were transfected with the 5SA mutant of YAP2 where five key regulatory S are mutated to A, rendering YAP2 constitutively active. As a control, we used the S94A YAP2 mutant that cannot interact with TEADs therefore abolishing YAP-induced gene expression [26]. Roflumilast treatment alone or in combination with vemurafenib decreased colony formation in A375R1 and SK-MEL-28R1 cells expressing the inactive 5SA-S94A YAP2 mutant. In contrast, roflumilast failed to inhibit cell growth in cells expressing the YAP 5SA mutant (Fig. 6D and E), demonstrating that PDE4 inhibition suppressed cell growth by inducing YAP phosphorylation and hence inhibiting the Hippo pathway.

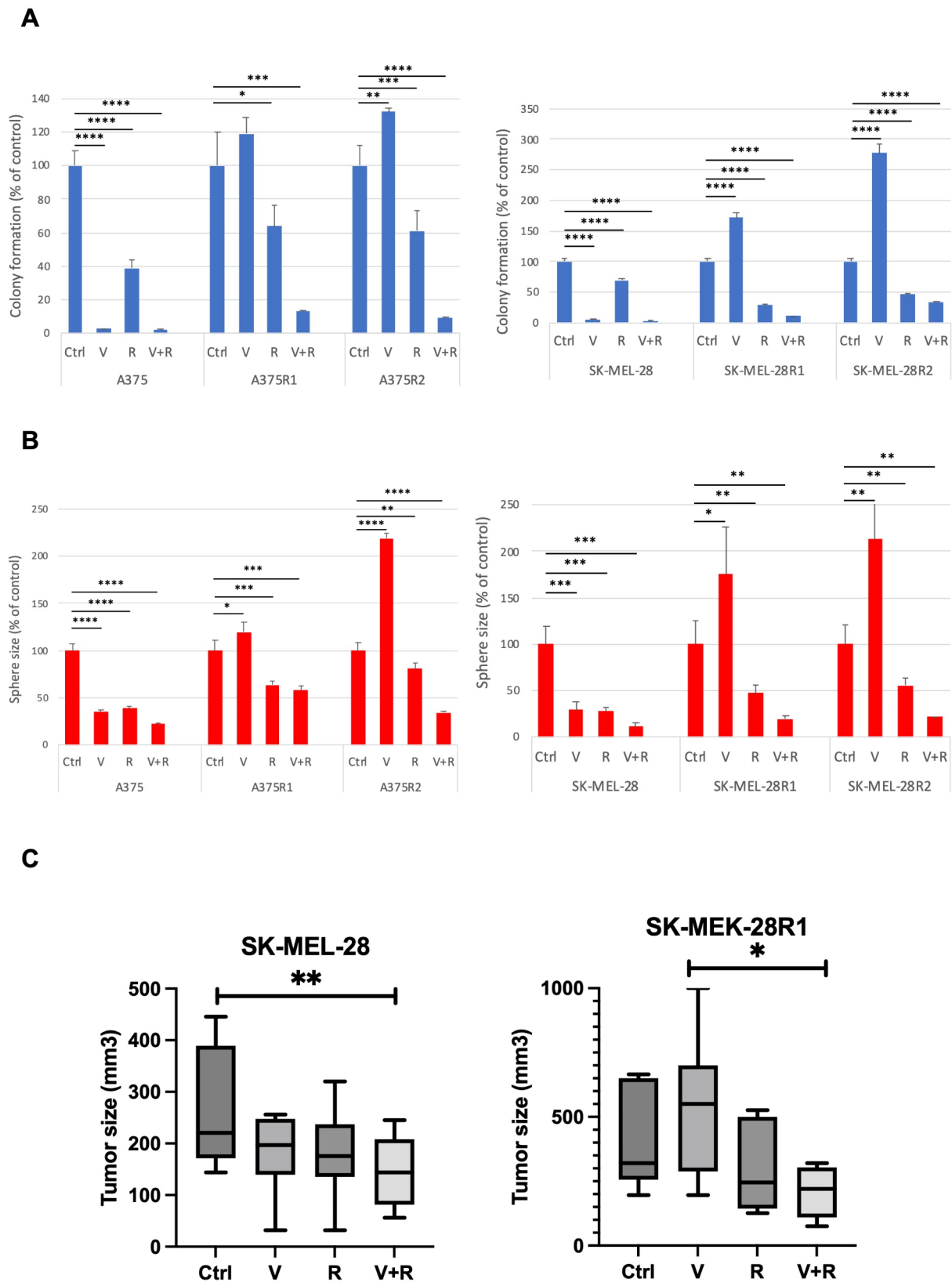


**Fig. 5** (See legend on next page.)

(See figure on previous page.)

**Fig. 5** PDE4 inhibition reduced cell proliferation in vitro and tumor growth in vivo of BRAF<sup>i</sup>-resistant melanoma cells. **A** A375, SK-MEL-28 their resistant derivatives (R1 and R2) were seeded in duplicate at low density and treated 3 times a week with DMSO (Ctrl), 10  $\mu$ M vemurafenib (V), 10  $\mu$ M roflumilast (R) or the combination of both inhibitors. After 2 weeks, cells were fixed, stained and the number of clones quantified. Bars represent mean $\pm$ -SD of 3 independent experiments. **B** A375, SK-MEL-28 their resistant derivatives (R1 and R2) were seeded in duplicate at low density in ultra-low-attachment plates and treated with DMSO (Ctrl), 1  $\mu$ M vemurafenib (V), 10  $\mu$ M roflumilast (R) or the combination of both inhibitors for 10 days. After 10 days, the spheroid size was measured. Bars represent mean  $\pm$  SD and results are representative of 3 independent experiments per line. **C** mice were inoculated subcutaneously with SK-MEL-28 or SK-MEL-28R1 and when the tumors volume reached 80 $\pm$ 30 mm<sup>3</sup> they were treated with control, vemurafenib (V), roflumilast (R) or the combination of both (V+R). The tumor size after three weeks of treatment is presented as mean $\pm$ -SD. \* $P$ <0.05, \*\* $P$ <0.01, \*\*\* $P$ <0.001, \*\*\*\* $P$ <0.0001; unpaired Student t-test

## Discussion

The cAMP signaling pathway is an essential regulator of many physiological processes such as proliferation, migration and angiogenesis. Because these processes are also involved in tumor growth, modulating cAMP level could be of great interest in the control of tumor proliferation. In general, basal cAMP concentrations are lower in many tumor cells compared to healthy cells and therefore increasing cAMP concentrations can slow down tumor cell growth and chemotaxis and increase differentiation or apoptosis in many cancer cells [27]. In melanoma, however, the cAMP pathway has been shown to have both tumor-promoting and tumor-suppressive properties as well as a role in sensitization and resistance to targeted therapy [28]. These discrepancies may be explained by differences in the duration as well as the localization of the cAMP signal which are regulated by the activity of both the adenylyl cyclase and the phosphodiesterase enzymes [29]. Amongst the family of phosphodiesterases, PDE4D is one of the PDE4 isoforms highly expressed in a variety of cancers. PDE4D was previously suggested as a potential oncogene in several human solid cancers, including breast cancer, hepatocellular carcinoma, pancreatic ductal adenocarcinoma, renal cell carcinoma and prostate tumors [30–35]. We have previously shown that PDE4D was overexpressed in advanced melanoma and metastases, and associated with worse prognosis [15]. In BRAF-mutated melanoma cell lines, PDE4D overexpression promoted invasion through its interaction with focal adhesion kinase via the scaffolding protein RACK1 [15]. The PDE4D gene was also found to be negatively associated with survival in patients with metastatic melanoma lesions using gene expression profiling [14].

In the present study, we explored the role of PDE4D in the resistance of BRAF-mutated melanoma to targeted therapy. We demonstrated in a panel of human BRAF-mutated melanoma biopsy samples that PDE4D expression in situ could separate short and long responders to MAPK inhibitors. We demonstrated a close association between PDE4D expression and poor prognosis in patients treated with MAPKi. For 2 patients for which we had biopsies before and after treatment, we observed that PDE4D expression increased upon treatment confirming the correlation between overexpression of PDE4D and resistance to treatment in vivo. We reproduced this

observation in two melanoma cell lines in which acquired resistance was associated with a markedly increased expression of PDE4D compared to parental cell lines.

The PDE4D locus codes for 9 different isoforms that differ in terms of the length and complexity of their N-terminal regulatory domains, which regulate substrate specificity, tissue expression profile and subcellular localization. This is important because isoform-specific targeting could enable selective restoration of cAMP signaling in affected compartments without disturbing cyclic nucleotide signaling elsewhere, avoiding side effects [11]. We identified the PDE4D5 isoform as the main isoform expressed in resistant melanoma cell lines as well as melanoma biopsies from resistant tumors. How PDE4D5 is expressed in resistant cells remains to be fully elucidated, but we postulate that demethylation of a CpG island upstream of the PDE4D5 promoter may explain the increase in PDE4D5 expression. In agreement, deletion of a fragment of chromosome 5 encompassing this CpG island in the SK-MEL-28 parental cell line was associated with high expression of PDE4D5. Moreover, microdeletions in the PDE4D locus, affecting only the intragenic regions of PDE4D, have been identified in a range of solid primary tumors and established cancer cell lines [30]. These microdeletions, affecting regions in the first exons, were associated with high PDE4D mRNA and protein expression. Finally, in the “Genomic Classification of Cutaneous Melanoma”, fusion of the PDE4D gene to multiple partner genes was identified in 5 samples [36]. In each case, the region encompassing the CpG island was removed by the fusion whereas the PDE4D catalytic domain remained intact. Altogether, these data suggest that expression of PDE4D, and in particular the PDE4D5 isoform, is restricted by epigenetic modification such as methylation upstream of the PDE4D5 promoter, and that removal of these epigenetic modifications or deletion of this inhibitory region allows PDE4D5 expression in tumors in general, and in melanoma in particular.

By regulating the cAMP pathway, PDE4D plays a major role in the cross-talk between the cAMP and the MAPK pathways which are essential in regulating the fate of melanocytes and melanoma [37]. cAMP-activated PKA exerts regulatory effects on components of the MAPK pathway, inhibiting RAF1 directly, whereas it can also activate BRAF, albeit indirectly [28]. Tumor cells

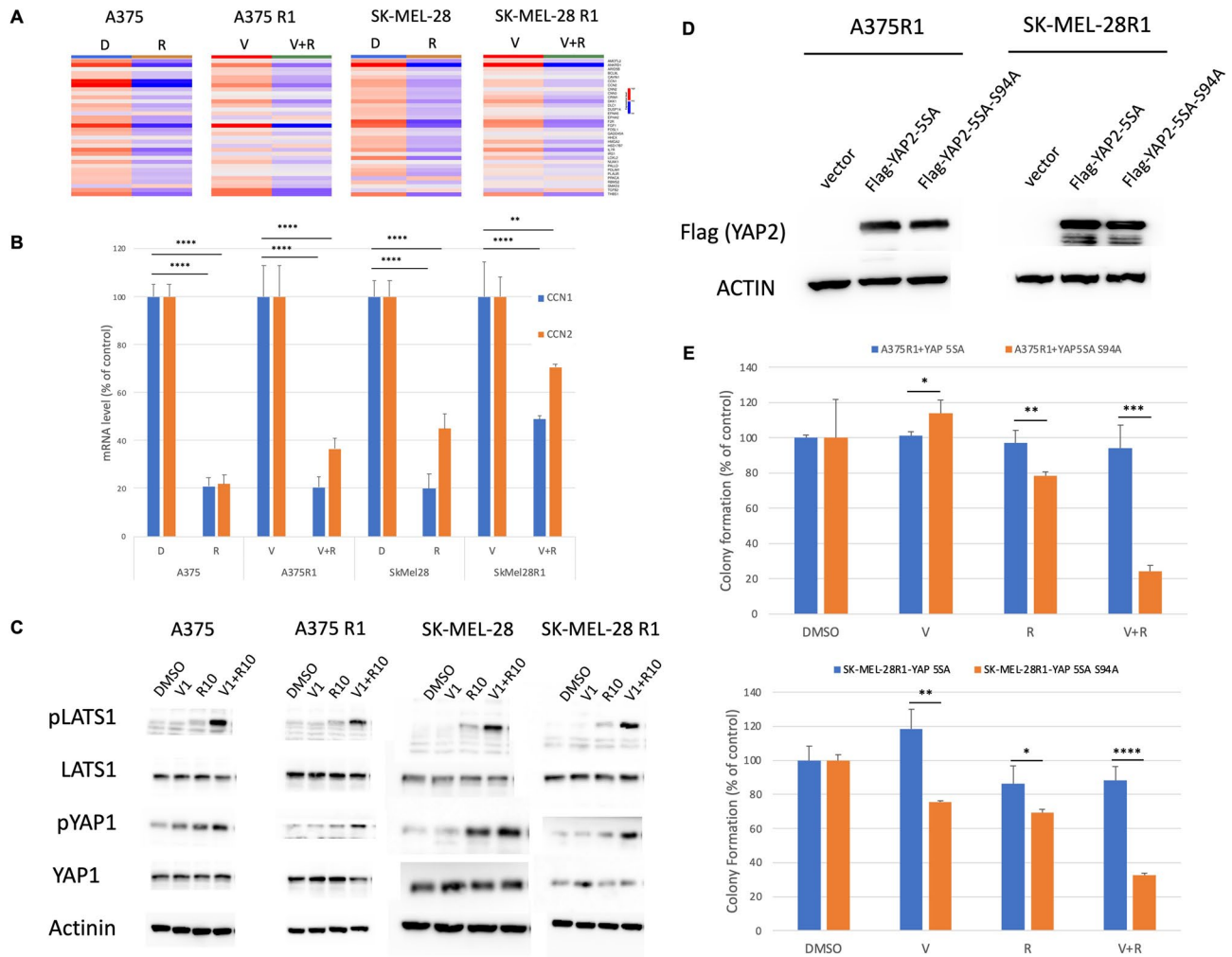


**Fig. 6** PDE4 inhibition suppresses melanoma growth through inactivation of the Hippo pathway. **A** A375, SK-MEL-28 and their resistant derivatives A375R1 and SK-MEL-28R1 were treated with vemurafenib 1  $\mu$ M (V), roflumilast 10  $\mu$ M (R) or the combination of both (V+R) for 24 h and the ARN extracted. The global expression of all mRNA was evaluated by RNAseq and the expression of a series of 34 genes from the hippo pathway in melanoma [24] showing differential expression in response to roflumilast (R) in the four cell lines is presented as a heat map. **B** mRNA level of CCN1 and CCN2 was quantified by quantitative by RT-PCR, normalized to GAPDH mRNA level, in A375, SK-MEL-28 and their resistant derivatives A375R1 and SK-MEL-28R1. Bars represent mean $\pm$ -SD and results are representative of 3 independent experiments per line. **C** A375, A375R1, SK-MEL-28 and SK-MEL-28R1 were treated with DMSO, vemurafenib 1  $\mu$ M (V1), roflumilast 10  $\mu$ M (R10) or the combination of both (V1 + R10) for 24 h. The effect on LATS1 phosphorylation (pLATS1), YAP1 phosphorylation (pYAP1) was measured by immunoblot, total LATS1, YAP1 and  $\alpha$ -ACTININ served as a loading control. **D** The level of YAP mutants in resistant A375R1 and SK-MEL-28R1 stably expressing the active mutant YAP 55A or the inactive mutant YAP 55A S94A was measured by immunoblot (Flag),  $\beta$ -ACTIN served as a loading control. **E** resistant A375R1 and SK-MEL-28R1 stably expressing the active mutant YAP 55A or the inactive mutant YAP 55A S94A were seeded in duplicate at low density and treated 3 time a week with DMSO, 10  $\mu$ M vemurafenib (V), 10  $\mu$ M roflumilast (R) or the combination of both inhibitors (V+R). After 2 weeks, cells were fixed, stained and the number of clones quantified. Bars represent mean $\pm$ -SD of 3 independent experiments. \* $P$  < 0.05, \*\* $P$  < 0.01, \*\*\* $P$  < 0.001, \*\*\*\* $P$  < 0.0001; unpaired Student t-test

exhibiting PDE4D overexpression and therefore cAMP depletion are incapable of PKA-mediated RAF1 inhibition allowing RAF isoform switching which is necessary to maintain ERK activation in tumor cells. We have previously shown that this RAF isoform switch induced by PDE4 overexpression happens in RAS-mutated melanoma [8, 9]. Similarly, we showed here that when BRAF activity is suppressed by inhibitors, MAPK is rewired to allow the development of acquired resistance by inducing RAF1-dependent ERK activation. PDE4D5

overexpression increased RAF1 activation, inducing partial resistance of the MAPK pathway to BRAF and MEK inhibitors. This led to an increase in drug-tolerant persister cells known to represent a major survival mechanism against BRAF and MEK inhibitor treatment in melanoma [38]. These cells will later become resistant cells by acquiring genetic alterations, such as RAS mutations, promoting a complete switch from BRAF to RAF1 isoform in resistant cells.

Besides the potential role of PDE4D as a predictive factor in resistance to targeted therapy, it could also represent a good candidate for therapy in resistant melanoma. Indeed, we found that PDE4 inhibition exhibited significant antitumor activity both *ex vivo* and *in vivo* against melanoma cell lines resistant to targeted therapies. In the present study, we demonstrated that roflumilast reduced the colony formation of three melanoma cell lines as well as their resistant derivatives. In the latter, the PDE4 inhibitor counteracted the pro-proliferative effect of the BRAF inhibitor. We confirmed these results on cells grown as spheroids where the combination of roflumilast and vemurafenib reduced sphere growth of resistant cell lines. Finally, we demonstrated that the combination of vemurafenib and roflumilast induced a significant reduction in tumor size *in vivo* in xenograft models. This is in agreement with our recent data showing a significant inhibition of proliferation of RAS mutated melanoma resistant to MEK inhibitors with the combination of roflumilast and cobimetinib [39]. The anti-proliferative effect of PDE4 inhibition has also been reported in other types of cancer such as hepatocellular carcinoma, lung, prostate, colorectal cancer and medulloblastoma [40–44]. In lung cancer, roflumilast was shown to act synergistically with platinum-based agents to induce apoptosis [45]. Similarly, roflumilast was shown to enhance cisplatin-induced cytotoxicity in prostate cancer cell lines [46]. Finally, Mishra et al. demonstrated that PDE4D played a pivotal role in acquired resistance of breast cancer to tamoxifen, and that combining PDE inhibition with tamoxifen suppressed tumor growth better than each drug alone [32].

To gain insight into the molecular mechanism of proliferation inhibition by PDE4 inhibition, we conducted an RNA-seq assay to identify signaling pathways modulated by roflumilast. We showed that roflumilast did not inhibit the MAPK pathway in resistant melanoma but instead modulated the Hippo/YAP pathway. This result implies that although PDE4D overexpression promotes a switch from BRAF to RAF1 isoform which favors drug-tolerant persister cells, once the cells become resistant, PDE4D overexpression becomes necessary to maintain resistance by activating the Hippo/YAP pathway. We confirmed the changes in expression of the canonical Hippo-pathway-dependent genes *CCN1* and *CCN2* by qRT-PCR in cells and in tumors treated with roflumilast. We further showed that increasing cAMP level with PDE4 inhibitor induced LATS1 phosphorylation which in turn phosphorylated YAP, inactivating it. Expression of a constitutively active mutant of YAP rescued the cells from proliferation inhibition confirming that PDE4 inhibition suppressed cell growth by inducing YAP phosphorylation and hence inhibiting the Hippo pathway in resistant cells. The Hippo/YAP signaling pathway plays a pivotal role

in tumorigenesis, and was also recently closely associated with the occurrence of resistance in melanoma [47]. These results are in agreement with recent work showing that cAMP acts as a tumor suppressor in a wide range of human cancers through inactivation of the Hippo protein YAP inside the nucleus [23].

## Conclusions

In conclusion, our study revealed that PDE4D is aberrantly over-expressed in resistant melanoma, where it is a predictor of a poor response to MAPKi. Moreover, inhibition of PDE4D blocked the growth of melanoma tumors *in vivo*, supporting the role of PDE4D as a novel player in resistance to BRAF and MEK inhibitors in melanoma, and a potential target for the treatment of resistant tumors. However, the use of PDE4 inhibitors in cancer therapy should be investigated with caution because cAMP exerts suppressive effects on B and T lymphocytes [48]. Nevertheless, recent data showed that roflumilast did not antagonize the clinical activity of checkpoint blockers in an *in vivo* syngeneic lymphoma model [49]. Moreover, data from the three roflumilast trials, which included more than 9000 patients with COPD, did not show an increase in lung cancer diagnosis [50] paving the way for the use of PDE4D inhibitors in cancer therapy.

## Abbreviations

a-MSH	Alpha-melanocyte stimulating hormone
cAMP	Cyclic AMP
MAPK	Mitogen-activated protein kinase
MAPKi	MAPK inhibitors
MC1R	Type 1 melanocortin receptor
PDE	Phosphodiesterases
PDE4D	Phosphodiesterase type 4D
PFS	Progression-free survival

## Supplementary Information

The online version contains supplementary material available at <https://doi.org/10.1186/s12964-024-01941-y>.

Supplementary Material 1

## Acknowledgements

We thank Jocelyne André and Elodie Voilin for their technical help. The authors thank Dr Kirsten Dumaz for proofreading the manuscript.

## Author contributions

Conceptualization: JD, CL, ND; Methodology: JD, SB, AR, BL, CRM, ND; Investigation: JD, SB, AR, BL, CRM, SM, CL, ND; Funding acquisition: CL, ND; Project administration: CL, ND; Supervision: SM, CL, ND; Writing – original draft: JD, SB, ND; Writing – review & editing: JD, SB, BL, SM, CL, ND. All authors read and approved the final manuscript.

## Funding

This work was supported by Institut National de la Santé Et de la Recherche Médicale (INSERM), Université Paris Cité, Ligue Nationale contre le Cancer (Grant n° GB/MA/CD/1Q -12642SB), Société Française de Dermatologie (SFD), Fondation ARC pour la Recherche sur le Cancer (Grant n° PJA 20131200216), Gefluc Paris – Ile de France.



**Data availability**

The datasets used and analysed during the current study are available from the corresponding author on reasonable request.

**Declarations****Ethics approval and consent to participate**

The cohort of patients with unresectable advanced melanoma identified from the French prospective MELBASE biobank at Saint-Louis hospital, Paris, were included (ClinicalTrials.gov identifier: NCT02828202, CPP Ile-de-France XI, number 12027, 2012). All patients had provided written informed consent prior to enrollment. For melanoma cell xenograft experiments, animal housing, handling and all procedures involving mice were performed in accordance to Directive 2010/63/EU and all protocols were approved by the Committee on the Ethics of Animal Experiments of the French Ministry of Agriculture (Permit Number: APAFIS#11775-2017101316112852 v2).

**Consent for publication**

Not applicable.

**Competing interests**

The authors declare no competing interests.

**Author details**

<sup>1</sup>Human Immunology Pathophysiology & Immunotherapy (HIPI), Université Paris Cité, INSERM U976 - Hôpital Saint Louis - 1 avenue Claude Vellefaux, Paris 75010, France

<sup>2</sup>Université Paris Cité, AP-HP Dermato-oncology and CIC, Cancer institute APHP,nord Paris Cité, INSERM U976, Saint Louis Hospital, Paris F-75010, France

<sup>3</sup>Department of Pharmacology and Tumor Genomics, Hôpital Saint Louis, Assistance Publique-Hôpitaux de Paris, Paris F-75010, France

Received: 25 June 2024 / Accepted: 11 November 2024

Published online: 21 November 2024

**References**

- Castellani G, Buccarelli M, Arasi MB, Rossi S, Pisanu ME, Bellenghi M et al. BRAF mutations in Melanoma: Biological aspects, therapeutic implications, and circulating biomarkers. *Cancers (Basel)*. 2023;15(16).
- Ugurel S, Rohmel J, Ascierto PA, Becker JC, Flaherty KT, Grob JJ, et al. Survival of patients with advanced metastatic melanoma: the impact of MAP kinase pathway inhibition and immune checkpoint inhibition - update 2019. *Eur J Cancer*. 2020;130:126–38.
- Patel M, Eckburg A, Gantiwala S, Hart Z, Dein J, Lam K et al. Resistance to molecularly targeted therapies in Melanoma. *Cancers (Basel)*. 2021;13(5).
- Riaud M, Maxwell J, Soria-Bretones I, Dankner M, Li M, Rose AAN. The role of CRAF in cancer progression: from molecular mechanisms to precision therapies. *Nat Rev Cancer*. 2024;24(2):105–22.
- Zhao J, Luo Z. Discovery of Raf Family is a milestone in deciphering the ras-mediated Intracellular Signaling Pathway. *Int J Mol Sci*. 2022;23(9).
- Busca R, Ballotti R. Cyclic AMP a key messenger in the regulation of skin pigmentation. *Pigment Cell Res*. 2000;13(2):60–9.
- Dumaz N, Hayward R, Martin J, Ogilvie L, Hedley D, Curtin JA, et al. In Melanoma, RAS mutations are accompanied by switching signaling from BRAF to CRAF and disrupted cyclic AMP Signaling. *Cancer Res*. 2006;66(19):9483–91.
- Dorard C, Estrada C, Barbotin C, Larcher M, Garancher A, Leloup J, et al. RAF proteins exert both specific and compensatory functions during tumour progression of NRAS-driven melanoma. *Nat Commun*. 2017;8:15262.
- Marquette A, Andre J, Bagot M, Bensussan A, Dumaz N. ERK and PDE4 cooperate to induce RAF isoform switching in melanoma. *Nat Struct Mol Biol*. 2011;18(5):584–91.
- Holcomb NC, Bautista RM, Jarrett SG, Carter KM, Gober MK, D'Orazio JA. cAMP-mediated regulation of melanocyte genomic instability: a melanoma-preventive strategy. *Adv Protein Chem Struct Biol*. 2019;115:247–95.
- Baillie GS, Tejada GS, Kelly MP. Therapeutic targeting of 3',5'-cyclic nucleotide phosphodiesterases: inhibition and beyond. *Nat Rev Drug Discov*. 2019;18(10):770–96.
- Schick MA, Schlegel N. Clinical implication of Phosphodiesterase-4-Inhibition. *Int J Mol Sci*. 2022;23(3).
- Hsien Lai S, Zervoudakis G, Chou J, Gurney ME, Quesnelle KM. PDE4 subtypes in cancer. *Oncogene*. 2020;39(19):3791–802.
- Bogunovic D, O'Neill DW, Belitskaya-Levy I, Vacic V, Yu YL, Adams S, et al. Immune profile and mitotic index of metastatic melanoma lesions enhance clinical staging in predicting patient survival. *Proc Natl Acad Sci U S A*. 2009;106(48):20429–34.
- Delyon J, Servy A, Laugier F, Andre J, Ortonne N, Battistella M, et al. PDE4D promotes FAK-mediated cell invasion in BRAF-mutated melanoma. *Oncogene*. 2017;36(23):3252–62.
- Jebali A, Battistella M, Lebbe C, Dumaz N. RICTOR affects Melanoma Tumorigenesis and its resistance to targeted therapy. *Biomedicines*. 2021;9(10).
- Le Jeune IR, Shepherd M, Van Heeke G, Houslay MD, Hall IP. Cyclic AMP-dependent transcriptional up-regulation of phosphodiesterase 4D5 in human airway smooth muscle cells. Identification and characterization of a novel PDE4D5 promoter. *J Biol Chem*. 2002;277(39):35980–9.
- Vallarelli AF, Rachakonda PS, Andre J, Heidenreich B, Riffaud L, Bensussan A, et al. TERT promoter mutations in melanoma render TERT expression dependent on MAPK pathway activation. *Oncotarget*. 2016;7(33):53127–36.
- Fang D, Nguyen TK, Leishear K, Finko R, Kulp AN, Hotz S, et al. A tumorigenic subpopulation with stem cell properties in melanomas. *Cancer Res*. 2005;65(20):9328–37.
- Ramgolam K, Lauriol J, Lalou C, Lauden L, Michel L, de la Grange P, et al. Melanoma spheroids grown under neural crest cell conditions are highly plastic migratory/invasive tumor cells endowed with immunomodulator function. *PLoS ONE*. 2011;6(4):e18784.
- Al Hmada Y, Brodell RT, Kharouf N, Flanagan TW, Alamodi AA, Hassan SY et al. Mechanisms of Melanoma Progression and Treatment Resistance: role of Cancer stem-like cells. *Cancers (Basel)*. 2024;16(2).
- Packer LM, East P, Reis-Filho JS, Marais R. Identification of direct transcriptional targets of (V600E)BRAF/MEK signalling in melanoma. *Pigment Cell Melanoma Res*. 2009;22(6):785–98.
- Drozd MM, Doane AS, Alkallas R, Desman G, Bareja R, Reilly M, et al. A nuclear cAMP microdomain suppresses tumor growth by Hippo pathway inactivation. *Cell Rep*. 2022;40(13):111412.
- Zhang X, Yang L, Szeto P, Abali GK, Zhang Y, Kulkarni A, et al. The Hippo pathway oncoprotein YAP promotes melanoma cell invasion and spontaneous metastasis. *Oncogene*. 2020;39(30):5267–81.
- Hong AW, Meng Z, Yuan HX, Plouffe SW, Moon S, Kim W, et al. Osmotic stress-induced phosphorylation by NLK at Ser128 activates YAP. *EMBO Rep*. 2017;18(11):72–86.
- Zhao B, Ye X, Yu J, Li L, Li W, Li S, et al. TEAD mediates YAP-dependent gene induction and growth control. *Genes Dev*. 2008;22(14):1962–71.
- Ahmed MB, Alghamdi AAA, Islam SU, Lee JS, Lee YS. cAMP signaling in Cancer: a PKA-CREB and EPAC-Centric Approach. *Cells*. 2022;11:13.
- Bang J, Zippin JH. Cyclic adenosine monophosphate (cAMP) signaling in melanocyte pigmentation and melanomagenesis. *Pigment Cell Melanoma Res*. 2021;34(1):28–43.
- Getz M, Rangamani P, Ghosh P. Regulating cellular cyclic adenosine monophosphate: sources, sinks, and now, tunable valves. *Wiley Interdiscip Rev Syst Biol Med*. 2020;12(5):e1490.
- Lin DC, Xu L, Ding LW, Sharma A, Liu LZ, Yang H, et al. Genomic and functional characterizations of phosphodiesterase subtype 4D in human cancers. *Proc Natl Acad Sci USA*. 2013;110(15):6109–14.
- Bottcher R, Dulla K, van Strijp D, Dits N, Verhoef EI, Baillie GS, et al. Human PDE4D isoform composition is deregulated in primary prostate cancer and indicative for disease progression and development of distant metastases. *Oncotarget*. 2016;7(43):70669–84.
- Mishra RR, Belder N, Ansari SA, Kayhan M, Bal H, Raza U, et al. Reactivation of cAMP pathway by PDE4D inhibition represents a Novel Druggable Axis for overcoming tamoxifen resistance in ER-positive breast Cancer. *Clin Cancer Res*. 2018;24(8):1987–2001.
- Liu F, Ma J, Wang K, Li Z, Jiang Q, Chen H, et al. High expression of PDE4D correlates with poor prognosis and clinical progression in pancreatic ductal adenocarcinoma. *J Cancer*. 2019;10(25):6252–60.
- Cao M, Nawalaniec K, Ajay AK, Luo Y, Moench R, Jin Y, et al. PDE4D targeting enhances anti-tumor effects of sorafenib in clear cell renal cell carcinoma and attenuates MAPK/ERK signaling in a CRAF-dependent manner. *Transl Oncol*. 2022;19:101377.

35. Ren H, Chen Y, Ao Z, Cheng Q, Yang X, Tao H, et al. PDE4D binds and interacts with YAP to cooperatively promote HCC progression. *Cancer Lett.* 2022;541:215749.
36. TCGA. Genomic classification of cutaneous melanoma. *Cell.* 2015;161(7):1681–96.
37. Khaled M, Levy C, Fisher DE. Control of melanocyte differentiation by a MITF-PDE4D3 homeostatic circuit. *Genes Dev.* 2010;24(20):2276–81.
38. Lim SY, Rizos H. Single-cell RNA sequencing in melanoma: what have we learned so far? *EBioMedicine.* 2024;100:104969.
39. Louveau B, De Reger C, Jouenne F, Sadoux A, Allayous C, Da Meda L et al. Combined PDE4+MEK inhibition shows antiproliferative effects in NRASQ61 mutated melanoma preclinical models. *Melanoma Res.* 2023.
40. Tsunoda T, Ota T, Fujimoto T, Doi K, Tanaka Y, Yoshida Y, et al. Inhibition of phosphodiesterase-4 (PDE4) activity triggers luminal apoptosis and AKT dephosphorylation in a 3-D colonic-crypt model. *Mol Cancer.* 2012;11:46.
41. Ge X, Milenkovic L, Suyama K, Hartl T, Purzner T, Winans A et al. Phosphodiesterase 4D acts downstream of Neuropilin to control hedgehog signal transduction and the growth of medulloblastoma. *Elife.* 2015;4.
42. Powers GL, Hammer KD, Domenech M, Frantskevich K, Malinowski RL, Bushman W, et al. Phosphodiesterase 4D inhibitors limit prostate cancer growth potential. *Mol Cancer Res.* 2015;13(1):149–60.
43. Yougbare I, Belemnaba L, Morin C, Abusnina A, Senouvo YF, Keravis T, et al. NCS 613, a potent PDE4 inhibitor, Displays Anti-inflammatory and Anti-proliferative properties on A549 lung epithelial cells and human lung Adenocarcinoma explants. *Front Pharmacol.* 2020;11:1266.
44. Ragusa F, Panera N, Cardarelli S, Scarsella M, Bianchi M, Biagioni S et al. Phosphodiesterase 4D Depletion/Inhibition exerts anti-oncogenic properties in Hepatocellular Carcinoma. *Cancers (Basel).* 2021;13(9).
45. Domvri K, Zarogoulidis K, Zogas N, Zarogoulidis P, Petanidis S, Porpodis K, et al. Potential synergistic effect of phosphodiesterase inhibitors with chemotherapy in lung cancer. *J Cancer.* 2017;8(18):3648–56.
46. Abdel-Wahab BA, Walbi IA, Albarqi HA, Ali FEM, Hassanein EHM. Roflumilast protects from cisplatin-induced testicular toxicity in male rats and enhances its cytotoxicity in prostate cancer cell line. Role of NF-kappaB-p65, cAMP/PKA and Nrf2/HO-1, NQO1 signaling. *Food Chem Toxicol.* 2021;151:112133.
47. Garcia-Rendueles MER, Krishnamoorthy G, Saqcena M, Acuna-Ruiz A, Revilla G, de Stanchina E, et al. Yap governs a lineage-specific neuregulin1 pathway-driven adaptive resistance to RAF kinase inhibitors. *Mol Cancer.* 2022;21(1):213.
48. Raker VK, Becker C, Steinbrink K. The cAMP pathway as therapeutic target in Autoimmune and Inflammatory diseases. *Front Immunol.* 2016;7:123.
49. Sasi B, Ethiraj P, Myers J, Lin AP, Jiang S, Qiu Z, et al. Regulation of PD-L1 expression is a novel facet of cyclic-AMP-mediated immunosuppression. *Leukemia.* 2021;35(7):1990–2001.
50. Wedzicha JA, Calverley PM, Rabe KF. Roflumilast: a review of its use in the treatment of COPD. *Int J Chron Obstruct Pulmon Dis.* 2016;11:81–90.

### Publisher's note

Springer Nature remains neutral with regard to jurisdictional claims in published maps and institutional affiliations.